MITSUBISHI ELECTRIC RESEARCH LABORATORIES
http://www.merl.com

A Comparison of Transient Heat Pump Cycle Simulations with Homogeneous and Heterogeneous Flow Models

Laughman, C.R.

TR2014-073 July 2014

Abstract

This paper compares two alternative approaches to the transient simulation of vapor-compression air-conditioning cycles that use different descriptions of the thermofluid behavior on the refrigerant side of the heat exchangers. While one of the most common modeling assumptions for two-phase refrigerant flow in transient cycle simulation is that the liquid and gas phases travel at the same velocity, a condition that is referred to as homogeneous flow, the two phases in real heat exchangers in vapor-compression cycles move at different velocities, requiring a heterogeneous flow model. Though both of these modeling approaches can be used to describe the transient cycle behavior, this paper demonstrates the extent to which the choice of the refrigerant flow model can have an impact on some of the aspects of the simulated cycle behavior, such as the heat exchanger mass inventory. These simulations are developed in the next-generation modeling language Modelica, which uses an acausal, equation-oriented approach to describe physical systems. The effect of the software implementation on the model performance is also discussed.

International Refrigeration and Air Conditioning Conference at Purdue

A Comparison of Transient Heat Pump Cycle Simulations with Homogeneous and Heterogeneous Flow Models

Christopher R. Laughman

Mitsubishi Electric Research Laboratories
Cambridge, MA 02139
laughman@merl.com

ABSTRACT

This paper compares two alternative approaches to the transient simulation of vapor-compression air-conditioning cycles that use different descriptions of the thermofluid behavior on the refrigerant side of the heat exchangers. While one of the most common modeling assumptions for two-phase refrigerant flow in transient cycle simulation is that the liquid and gas phases travel at the same velocity, a condition that is referred to as homogeneous flow, the two phases in real heat exchangers in vapor-compression cycles move at different velocities, requiring a heterogeneous flow model. Though both of these modeling approaches can be used to describe the transient cycle behavior, this paper demonstrates the extent to which the choice of the refrigerant flow model can have an impact on some of the aspects of the simulated cycle behavior, such as the heat exchanger mass inventory. These simulations are developed in the next-generation modeling language Modelica, which uses an acausal, equation-oriented approach to describe physical systems. The effect of the software implementation on the model performance is also discussed.

1 INTRODUCTION

Dynamic models of HVAC&R systems are widely applicable for a variety of different purposes, including component design and optimization, system-level design and optimization, controls development, and fault detection and diagnostics, and there has correspondingly been a wealth of research into different modeling approaches over the last 30 years (Rasmussen (2012), Li *et al.* (2014b)). This variety of different modeling methods arises due to the fact that the requirements that are placed upon a system model and the different assumptions that are made in the formulation of the model depend heavily on the eventual model application. For example, some applications may only require a steady-state lumped-parameter model that runs on a 8 MHz PowerPC machine and is only expected to have ±10% accuracy, while other applications may require the development of dynamic distributed-parameter models that are expected to run on a 2.5 GHz machine.

While there are a variety of types of dynamic cycle models, those which incorporate distributed parameter representations of heat exchanger behavior are particularly useful for describing spatially dependent phenomena, such as the effect of nonuniform air velocities over the surface of the heat exchanger, or the branching and joining of refrigerant pipes as a result of particular circuiting configurations. Such detailed models are useful for understanding and constructing algorithms for the detection of changes in the behavior of the overall cycle, including the development of fault detection and diagnostic (FDD) methods for a variety of purposes, e.g., detecting refrigerant overcharge or leakage from a cycle.

The equation-oriented modeling language Modelica (Modelica Association, 2014), (Li *et al.*, 2014a) has been gaining in popularity for the modeling of complex thermofluid systems due to its ability to encode detailed descriptions of multiphysics problems in a software representation, its inherently object-oriented construction, and the fact that it is an open language. Moreover, the ability to encode behavioral models into specific objects provides the user with a powerful abstraction concept, as models can be created so that different physical effects, such as the effect of gravitational head or viscous dissipation, can be easily added to or removed from models. Like other equation-oriented modeling software, it uses a behavioral modeling paradigm (Willems, 2007), and employs computer algebra techniques to simplify and solve systems of differential algebraic equations (DAEs), such as those that represent the behavior of of heat exchangers, to produce a set of ordinary differential equations that can be simulated with state-of-the-art solvers, such as DASSL and Radau IIa (Cellier and Kofman, 2006).

In using Modelica to develop distributed-parameter models of the transient behavior of thermofluid systems, one of the many decisions that must be made is that of the manner for describing the two-phase flow pattern. One common assumption in the simulation of two-phase flow systems is that both phases flow at the same velocity, which is otherwise referred to as homogeneous flow pattern, while the relaxation of this assumption results in different phasic velocities, or a heterogeneous flow pattern, as discussed in Ghiaasiaan (2007) and Ishii and Hibiki (2011). These different flow patterns can affect the dynamics of a thermofluid system in a variety of different ways; in general, one of the most significant effects of the flow pattern in vapor compression cycles is that models with an assumption of homogeneous flow tend to result in lower predictions of mass inventory in two-phase heat exchangers than are typically seen in experiments, while heterogeneous flow models generally describe the mass inventory more accurately.

Much of the extant literature describing distributed parameter models of vapor compression systems in Modelica, such as that published by Casella (2006), Bonilla *et al.* (2012), and Mortada *et al.* (2012), assumes that the both phases of the refrigerant move at the same velocity. While this is a reasonable assumption for homogeneous dispersed flow (e.g., bubbly and spray flow), it is generally not valid for heterogeneous separated flow (e.g., stratified and annular flow) since for these systems (Kolev, 2005, p.151),

$$1 \leq \left(\frac{v_G}{v_L}\right) \leq \sqrt{\frac{\rho_L}{\rho_G}}. \tag{1}$$

One particularly predominant type of these heterogeneous flow models, referred to as a slip flow model, is that in which it is assumed that mass transfer across the phasic interface takes place without an accompanying momentum transfer. This flow model can be formulated as a set of equations describing the two-phase mixture, with an extra set of closure relations to relate the different phasic properties.

There has been some prior work in using Modelica to develop slip flow models of heat exchangers that are typically used in vapor compression systems. In his M.S. thesis, Bauer (1999) developed two different slip flow models for the dynamics of a evaporator, using both a static and a dynamic relation to describe the interactions between the phases. These models were validated on a shell-in-tube heat exchanger, with R22 as the working fluid and ethanol as the secondary fluid. The results from this work demonstrated that that the homogeneous flow modeling approach was inadequate to describe the evaporator's mass inventory, and that the performance of the static balance and the dynamic balance were comparable. More recently, Kærn (2011) coupled a slip-flow evaporator model to a moving-boundary condenser model and static compressor and expansion valve models to explore and understand the effects of maldistribution in evaporator coils.

This paper has two principal objectives. First, a set of distributed parameter models of the vapor compression cycle with both homogeneous flow and slip flow models is developed to describe the dynamics of the mass inventory of the heat exchangers to better understand and demonstrate the effect of the flow model on the distribution of refrigerant mass throughout the cycle. Second, this paper investigates the effect of the flow model on the equilibrium operating point of the two different heat exchangers, to better ascertain the impact of these modeling assumptions on the cycle dynamics. These objectives are accomplished via the development of Modelica models of both homogeneous and slip flow for heat exchangers with both boiling and condensing flows, as well as the integrations of these flow models into two otherwise identical cycles.

Section 2 of this paper contains descriptions of the finite control volume models of the heat exchangers with a formulation of the slip flow terms, as well as the component models required to develop a complete cycle model. Salient details of the implementation in Modelica are then described in Section 3, while Section 4 illustrates some salient results from complete cycle simulations to illustrate the differences between the two modeling approaches. Finally, conclusions and potential areas of further exploration are discussed in Section 5.

2 MODEL DESCRIPTION

A vapor compression cycle model requires component submodels for the heat exchangers, compressor, and expansion valve. Because of the complexity of the two-phase flow model, this section begins by describing the relations between the phasic and mixture fluid properties in a control volume, and this is followed with a discussion of the conservation equations for a control volume. These models are then combined to form a set of equations that characterize the

behavior of the heat exchangers. Finally, the models of the compressor and expansion valve are described at the end of this section.

The underlying physical dynamics of the refrigerant flow through the heat exchangers is governed by a set of partial differential equations (PDEs), which interrelate the mass, momentum, and energy balances in the fluid. Because of the difficulty of solving these PDEs in general, the research in this paper discretizes the PDEs, which results in a set of nonlinear ODEs that must be solved with a numerical integration routine. These balance equations do not completely define the set of equations, however; algebraic equations of state are needed to describe the relations between the thermodynamic and transport properties of the fluid, and experimentally derived closure relations are also needed to define some of the important interactions, such as the relationship between the heat flux and the temperature difference. This full set of mathematical relations can be seen to be a set of DAEs.

A number of assumptions were made in the construction of the heat exchanger model, including the fact that there are no gradients in either the refrigerant properties or the velocity field in the radial or θ directions, that each control volume is in thermodynamic equilibrium, that there is no thermal conduction along either the refrigerant or the heat exchanger wall in the z direction, that the wall temperature in each control volume is uniform, that the potential energy change across the heat exchanger is negligible, and that the air can be modeled as an ideal gas.

For a given volume containing two-phase refrigerant in the pipe, an extensive property Ψ can be written as the mass-weighted mixture of the constituent phasic properties by averaging over the phasic volumes, e.g.,

$$\Psi = \Psi_G + \Psi_L \tag{2}$$

$$\psi = \Psi/M_{total} = \psi_g M_g + \psi_L M_L \tag{3}$$

$$\psi = x\psi_G + (1-x)\psi_L \tag{4}$$

where x is referred to as the static quality, or

$$x = \frac{M_G}{M_G + M_L} = \frac{M_G}{M_{total}} \tag{5}$$

The same intensive property ψ can also be written as

$$\psi\rho V = \psi_G\rho_G V_G + \psi_L\rho_L V_L \tag{6}$$

$$\psi\rho = \gamma\psi_G\rho_G + (1-\gamma)\psi_L\rho_L \tag{7}$$

where the void fraction γ can be written as

$$\gamma = \frac{V_G}{V_G + V_L} = \frac{A_G}{A_G + A_L} \tag{8}$$

and the second equality applies when computing the void fraction over a control volume with a fixed length. This formulation of the property relations assumes that flow field containing both phases at z_0 is frozen at a point in time, and the spatial average that can be taken over this frozen flow field is also representative of the ensemble average at this point taken over a period of time (Ishii and Hibiki, 2011).

These expressions make it possible to write down aggregate intensive properties in terms of their phasic components, either in terms of the void fraction,

$$\rho = \gamma\rho_G + (1-\gamma)\rho_L \tag{9}$$

or the static quality,

$$h = xh_G + (1-x)h_L \tag{10}$$

$$u = xu_G + (1-x)u_L \tag{11}$$

$$v = xv_G + (1-x)v_L. \tag{12}$$

A relation between the void fraction and the static quality can also be formulated by noting that

$$x = \frac{M_G}{M_{total}} = \frac{\rho_G V_G}{\rho V} = \gamma \frac{\rho_G}{\rho} \tag{13}$$

and similarly

$$(1 - x) = (1 - \gamma)\frac{\rho_L}{\rho}. \tag{14}$$

Because it will be used in the energy balance, it is also helpful to define a quantity referred to as the flow quality $\dot{x}$ to describe the ratio of the phasic mass flow rates, e.g.,

$$\dot{x} = \frac{\dot{m}_G}{\dot{m}_G + \dot{m}_L} \tag{15}$$

$$= \frac{\gamma \rho_G v_G}{\gamma \rho_G v_G + (1 - \gamma)\rho_L v_L} \tag{16}$$

$$= \frac{x v_G}{x v_G + (1 - x) v_L}. \tag{17}$$

It is clear from Equation 16 that the static quality is equal to the flow quality only when the gas and liquid velocities are equal. It is also helpful to express the void fraction γ in terms of the flow quality, e.g.,

$$\frac{1}{\gamma} = 1 + \left(\frac{1 - \dot{x}}{\dot{x}}\right)\left(\frac{v_G}{v_L}\right)\left(\frac{\rho_G}{\rho_L}\right). \tag{18}$$

The states that are chosen for the system are the pressure and the *in situ*, or density-weighted, enthalpy, based upon the frozen flow field (Equation 10). This *in situ* enthalpy differs from the "mixed-cup", or flow-weighted, enthalpy, which is defined as

$$\dot{m}\bar{h} = \dot{m}_G h_G + \dot{m}_L h_L \tag{19}$$

$$\bar{h} = \dot{x} h_G + (1 - \dot{x}) h_L, \tag{20}$$

Both of these different enthalpies will appear separately in the conservation equations, and are only equal if $x = \dot{x}$.

By using these property relations, the mass, momentum, and energy balance equations can be written down for the two-phase medium using the mixture properties, as described above. These balance equations for each one-dimensional individual control volume can be formulated in a relatively straightforward manner under a homogeneous flow assumption, as discussed in White (2008) and in Franke *et al.* (2009b) for a more Modelica-specific context, are

$$\frac{\partial(\rho A)}{\partial t} + \frac{\partial(\rho A v)}{\partial x} = 0 \tag{21}$$

$$\frac{\partial(\rho v A)}{\partial t} + \frac{\partial(\rho v^2 A)}{\partial x} = -A\frac{\partial p}{\partial x} - F_f \tag{22}$$

$$\frac{\partial(\rho(u + v^2/2)A)}{\partial t} + \frac{\partial(\rho v(h + v^2/2)A)}{\partial x} = \frac{\partial Q}{\partial x}, \tag{23}$$

The friction force F_f, is equal to the product of the cross-sectional area at location z_0 multiplied by the equivalent pressure drop due to friction (Equation 24),

$$\Delta p_{fric} = \zeta \frac{L}{D}\frac{\rho v^2}{2} \tag{24}$$

where the dimensionless friction factor ζ is developed through a correlation (Stephan, 2010).

An alternative energy balance Elmqvist *et al.* (2003) can be formed by multiplying the momentum balance by the fluid velocity v and subtracting it from the original energy balance, resulting in

$$\frac{\partial(\rho u A)}{\partial t} + \frac{\partial(\rho v h A)}{\partial x} = vA\frac{\partial p}{\partial x} + vF_f + \frac{\partial Q}{\partial x}. \tag{25}$$

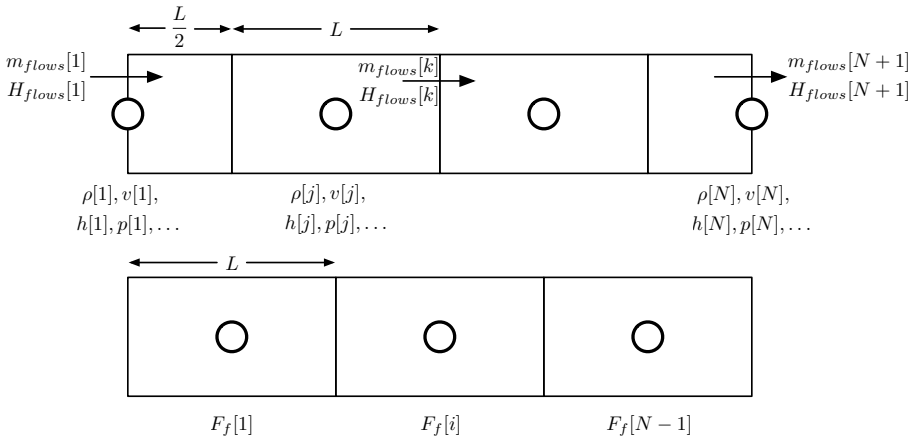

Figure 1: The staggered grids used to solve the balance equations.

This formulation is useful because it only includes the derivative of internal energy with respect to time; all other derivatives are spatial. This particular discretization of this PDE therefore will be much easier to express as an ODE than would otherwise be the case, since only derivatives of the internal energy with respect to the state variables are necessary.

A distinction must be drawn between the above formulation of the balance equations for an element of fluid, which has boundaries that can deform over time, and the balance equations for a fixed control volume, which has stationary boundaries. The balance equations can be converted between both frames of reference by using the Reynolds transport theorem, e.g.,

$$\frac{d\Psi}{dt} = \int_V \frac{\partial(\rho\psi)}{\partial t} dV + \int_A \rho\psi(\tilde{\mathbf{v}}_\mathbf{B} \cdot \hat{\mathbf{n}}) dA \tag{26}$$

Moreover, it is important to choose the proper state variables with which to describe the balance equations for each of these fixed control volumes. The state variables chosen for these models are the pressure p and the *in situ* enthalpy h, since the equation of state for the medium can be represented in these coordinates over the entire thermodynamic space. Expressions for the mass and total internal energy in a given fixed control volume can therefore be written as

$$\frac{d(\rho V)}{dt} = V\left(\frac{\partial\rho}{\partial p}\frac{dp}{dt} + \frac{\partial\rho}{\partial h}\frac{dh}{dt}\right) \tag{27}$$

$$\frac{d(u\rho V)}{dt} = \frac{d(\rho h - p)V}{dt} = V\left(\frac{\partial\rho}{\partial p}h - 1\right)\frac{dp}{dt} + V\left(\frac{\partial\rho}{\partial h}h + \rho\right)\frac{dh}{dt} \tag{28}$$

The balance equations for fixed control volumes are solved on two staggered grids, as illustrated in Figure 1, to avoid the non-physical oscillatory solutions described in Patankar (1980). The mass and energy balances are solved on the upper grid, referred to as the thermal grid, while the momentum balance is solved on the lower grid, which is referred to as the momentum grid. This "staggered grid" approach is also helpful because the centers of the upper grids are aligned with the boundaries of the lower grid, so it is not necessary to interpolate properties to find the consistent values on the edges of the momentum grid. It is important to note that there are $i = j - 1$ volumes with j edges on the momentum grid.

The mass balance is only solved on the thermal grid, since all of its variables reside on this grid. Each control volume (CV) of the heat exchanger model will have mass flowing in and out of it; under the assumption that we have j control volumes and $k = j + 1$ boundaries around those control volumes, and since the mass flow rate of refrigerant across a boundary can be written $m_{flows} = \rho A v$, the mass balance equation can be written

$$\frac{d(\rho_j V_j)}{dt} = m_{flows,k} - m_{flows,k+1}, \tag{29}$$

where the length of integration over the control volume L enters the time derivative on the left hand side, i.e., $V = LA$. The fluid properties, e.g., ρ_j, u_j, p_j, are evaluated in the center of each cell. It is important to note that the mass flow rates m_{flows} are explicitly solved for on each boundary; this avoids the practice of evaluating the densities at the boundaries, rather than the middle of the cells.

The momentum balance equation can be written in a method similar to the mass balance, resulting in

$$\begin{aligned} \frac{d(m_{flows,i}l)}{dt} &= \rho_j v_j^2 A_j - \rho_{j+1} v_{j+1}^2 A_{j+1} + \\ &\quad \frac{A_j + A_{j+1}}{2}(p_{j+1} - p_j) + F_{f,i}, \end{aligned} \tag{30}$$

where the variables with the j index are referred to the energy grid, and the variables with the i index are referred to the momentum grid. Note that the friction force $F_{f,i}$ is calculated on the momentum grid because it is related to the mass flow rates $m_{flows,i}$ and the pressure difference between the centers of the adjacent thermal grid $p_{j+1} - p_j$.

The energy balance can also be written for the thermal grid,

$$\begin{aligned} \frac{\partial(\rho_j u_j A_j)}{\partial t} &= H_{flows,k} - H_{flows,k+1} + v_j A_j (p_{j+1} - p_j) + \\ &\quad v F_{f,i} + Q_{flows,j}, \end{aligned} \tag{31}$$

where the values of H_{flows} are also computed at the edges of the control volume using the mass flow rates and the upstream convected mixed-cup enthalpy, e.g.,

$$H_{flows,k} = m_{flows,k} \bar{h}_{upstream,j}, \tag{32}$$

and the particular value of mixed-cup enthalpy that is upstream is dependent on the flow direction. For the homogeneous flow model, this is identical to the *in situ* enthalpy, but these are not equivalent in the slip flow model.

While the above discussion was focused primarily on the refrigerant-side of the heat exchanger, the same approach was used to model the air-side of the heat exchanger, with the same mass, momentum, and energy balances. While the refrigerant-side models use complex equations of state to accurately describe the two-phase behavior, an ideal gas medium model for the air was used because there are no phase changes. This cross-flow heat exchanger was designed in a straightforward manner, and uses a large ideal mixing volume to distribute the air evenly to all of the channels on the air-side of the heat exchanger.

The refrigerant wall is modeled as one-dimensional heat conduction in the direction perpendicular to the refrigerant flow, with convective boundary conditions described by the refrigerant-side and air-side heat transfer coefficients, which will be given in Section 3. This wall element can be modeled simply by

$$\frac{d(m_w c_w)}{dt} = \frac{k_w A_s (T_a - T_w)}{L_w/2} + \frac{k_w A_s (T_b - T_w)}{L_w/2} \tag{33}$$

The compressor model assumes there is no mass or energy storage, so the relations between the inlet and outlet mass flow rates, pressures, and specific enthalpies are nonlinear and algebraic. These are given by the following standard types of relations,

$$\dot{m}_{comp} = \eta_v \rho_{suc} V f \tag{34}$$

$$h_{suc} = h_{suc} + \frac{h_{dis,isen} - h_{suc}}{\eta_{is}} \tag{35}$$

$$h_{dis,isen} = f(p_{suc}, h_{suc}), \tag{36}$$

where the functions η_v and η_{is} are calculated via compressor maps, and the isentropic enthalpy $h_{dis,isen}$ is calculated via the appropriate equation of state.

Lastly, a simple isenthalpic model of the expansion valve is used to describe the expansion process, with neither mass nor energy storage. The mass flow rate through the expansion device is related to the user-controlled size of the orifice in the valve, which ranged from 0 counts to 500 counts, as well as the density at the inlet of the valve and the pressure drop across the valve, e.g.,

$$\dot{m}_{EEV} = \theta(u)\sqrt{\rho_{in}(p_{in} - p_{out})}. \tag{37}$$

3 IMPLEMENTATION

In principle, the system of mixture equations discussed in Section 2 describes the thermofluid dynamics for both homogeneous flow and slip flow, where the slip flow model also contains an additional closure relation that defines the slip ratio in terms of other thermodynamic variables. In practice, however, such an implementation is not computationally practical, because of the discontinuities between the single phase and two-phase regions. For example, the calculation of the slip ratio v_G/v_L will go to infinity in the superheated region, which will either cause problems with numerical robustness, elicit the development of complex techniques to activate or deactivate particular equations, or some combination thereof.

One approach that addresses these discontinuities was proposed by Bauer (1999), in which the mean velocity v and the velocity difference Δv are used to calculate the balance equations, rather than the phasic velocities. This is done by using the expression for the mixture velocity (Equation 12) to formulate a new expression for the phasic velocities, e.g.,

$$v_G = v + (1-x)(\Delta v) \tag{38}$$
$$v_L = v - x(\Delta v). \tag{39}$$

This makes it possible to express the phasic mass flow rates in terms of v and Δv,

$$\dot{m}_G = \gamma\rho_G v_G A \tag{40}$$
$$= xv\rho A + x(1-x)(\Delta v)\rho A \tag{41}$$
$$= x\dot{m} + \dot{m}_{corr} \tag{42}$$
$$\dot{m}_L = (1-x)\dot{m} - \dot{m}_{corr}, \tag{43}$$

where $\dot{m}_{corr} = x(1-x)(\Delta v)\rho A$, and is calculated at the centers of each element of the thermal grid, as are all of the other thermodynamic properties. This can also be used to develop the following relation between x and $\dot{x}$,

$$\dot{x} = x + x(1-x)\frac{\Delta v}{v}. \tag{44}$$

This reformulation of the phasic velocities is particularly useful because the term proportional to Δv goes to zero both when $x \leq 0$ and when $x \geq 1$. The balance equations can be rewritten by using these expressions; the correspondingly reformulated mass balance for a fixed control volume is

$$\frac{dM}{dt} = \dot{m}_{G,in} + \dot{m}_{L,in} - \dot{m}_{G,out} - \dot{m}_{L,out} \tag{45}$$
$$\frac{d(\rho_j V_j)}{dt} = m_{flows,k} - m_{flows,k+1}, \tag{46}$$

while the modified momentum balance for the fixed control volume can be written as

$$\frac{dI}{dt} = \dot{I}_{in} - \dot{I}_{out} + (P_{in} - P_{out})A + F_f \tag{47}$$
$$\frac{d(m_{flows,i}l)}{dt} = \rho_j v_j^2 A_j + \dot{m}_{corr,j}(\Delta u)_j - \rho_{j+1}v_{j+1}^2 A_{j+1} - \dot{m}_{corr,j+1}(\Delta u)_{j+1} + \frac{A_j + A_{j+1}}{2}(p_{j+1} - p_j) + F_{f,i}, \tag{48}$$

and finally the energy balance for the fixed control volume can be rewritten as

$$\frac{dU}{dt} = \dot{m}_{in}\bar{h}_{in} - \dot{m}_{out}\bar{h}_{out} + \dot{Q} \tag{49}$$
$$\frac{d(\rho_j u_j A_j)}{dt} = H_{flows,k} - H_{flows,k+1} + v_j A_j(p_{j+1} - p_j) + vF_{f,i} + \dot{Q}_{flows,k} \tag{50}$$

where H_{flow} is again computed using the mixed-cup enthalpy, rather than the *in situ* enthalpy. While the mass and energy balances look identical to the homogeneous flow mixture equations, the phasic velocities will differ due to the non-unity slip ratio.

A variety of correlations are needed to close the system of equations. Because many widely used correlations are highly nonlinear with respect to some of the variables in the simulation, a set of simplified correlations were used instead to reduce both the complexity of the Modelica models and the time required to initialize and simulate the models. The same correlations were used for both cycle models. A number of other software development approaches proved

Type of correlation	Correlation used
Refrigerant-side heat transfer	Constant coefficient (α = 600)
Air-side heat transfer	Enhanced Gnielinski finned tube (Stephan, 2010)
Refrigerant-side pressure drop	Blasius/Hagen-Poiseuille interpolation (Elmqvist *et al.*, 2003)
Air-side pressure drop	Blasius/Hagen-Poiseuille interpolation (Elmqvist *et al.*, 2003)
Slip ratio	Zivi (1964)

Table 1: Correlations used to construct cycle models.

to be crucial to the successful operation of these models. These codes were developed by leveraging the relatively new `stream` operator in Modelica (Franke *et al.*, 2009a), which is generally used in models that involve the convective transport of properties, and makes them easier to initialize when the sign of the mass flow rate with respect to a component is not known *a priori*. This operator effectively generates two sets of connection equations for every component port, one for mass flow in each direction; the compiler is then able to dynamically choose which set of equations to use when solving for the mass flow rate. In addition, the `smooth` and `noEvent` operators (Modelica Association, 2014) in Modelica were also important, because they provided a signal to the compiler when it could differentiate expressions to reduce the index of the model DAEs. Finally, unit tests were extensively utilized to troubleshoot individual models and to identify consistent sets of initial conditions when these models were combined into larger systems.

4 RESULTS

The models described above were implemented using the Modelica compiler Dymola 2014 and tested extensively on a set of cycle models that used R410a as a working fluid from the commercially available Air-Conditioning Library (kn:, 2014). Each of these models was initialized from the same set of starting pressures, air-side temperatures, and mass flow rates, to ensure a valid basis for comparison. To illustrate the differences between these two models, one set of experiments is illustrated in Figures 2 and 3. At t=100 seconds during this experiment, the compressor speed was increased by a step from 49 Hz to 69 Hz, and the expansion valve was also opened from 50 counts to 70 counts.

It is evident from Figure 2 that there is a significant difference between the total mass inventory of the cycles with the alternative flow models. Though the two cycle models were initialized at exactly the same operating point, and have the same mass flow rate, the cycle with the homogeneous flow model has a total refrigerant charge of 0.524 kg of R410a, while the cycle with the slip flow model has a total refrigerant charge of 0.729 kg of R410a, resulting in a 40% larger charge. These large differences in charge are due in part to the fact that the liquid phase velocity is much lower than the vapor phase velocity, causing the total residence time of the liquid in the heat exchangers is much longer for the slip flow cycle than for the homogeneous flow cycle.

Figure 3 demonstrates the similarity between the pressure difference across the evaporator and the shape of the pressure transient caused by the change in the actuators, suggesting that not all of the dynamics of the system are not dependent upon the slip flow model. This result is encouraging, as it is similar to previous work in the modeling of evaporators. It is notable, however, that while the pressure drop across the condenser is similar in both flow models, the condenser inlet pressure is lower for the slip flow cycle (2844 kPa) than it is for the homogeneous flow model (2987 kPa). This suggests that the change in the total cycle charge due to the slip flow model does have an effect on some, but not all, of the thermodynamic variables (e.g., pressures) in the cycle. This is caused by the fact that the equilibrium state reached by the cycle is dependent upon the modeling assumptions made, again suggesting that the use of a slip flow model is important when it is applicable.

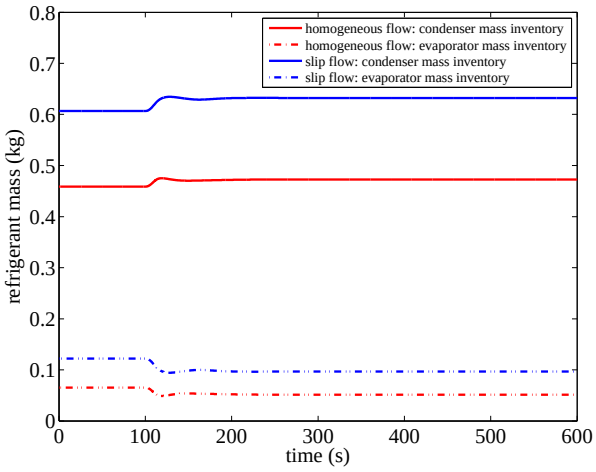

Figure 2: Heat exchanger refrigerant mass inventories for both cycle models.

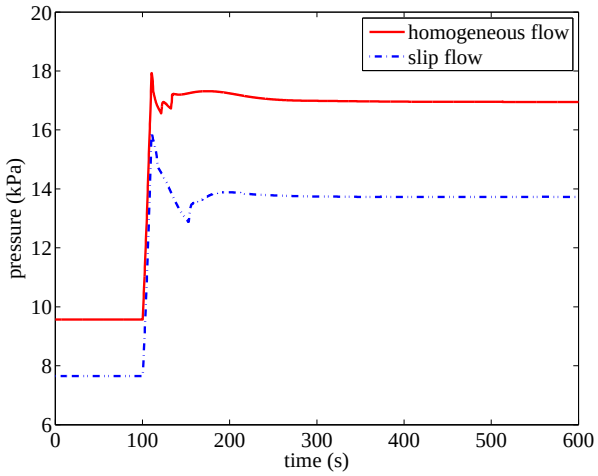

Figure 3: Pressure drop across the evaporator for both cycle models.

5 CONCLUSIONS AND FUTURE WORK

In this paper, a heterogeneous slip flow model for two-phase heat exchangers was proposed, and a Modelica implementation of two complete cycle models with different flow assumptions were discussed. Many of the features of Modelica, such as its non-causal modeling and object-oriented design paradigms, were essential to the development of these models. In comparing the characteristics of these two cycle models it is clear that the slip flow cycle model has a much higher refrigerant mass inventory than the homogeneous model, even though the evaporator pressure dynamics of both models are similar. On this basis of these results, it may reasonably be concluded that a cycle model using a homogeneous flow assumption that is calibrated against measurements of the system pressures will likely have significant errors in the predicted system charge. Further work in this area could include the validation of the complete cycle data against an experimental heat pump system, as well as the further refinement of these models, such as incorporation of more accurate correlations into the Modelica models.

NOMENCLATURE

A	cross-sectional area	k	thermal conductivity	**Subscript**	
D	tube diameter	$\dot{m}$	mass flow rate	k, i, j	control volume index
F	force	p	pressure	$dis, isen$	isentropic discharge
I	momentum	u	specific internal energy	suc	suction port
L	wall thickness	v	velocity	dis	discharge port
M	mass	x	static quality	G	gas
Q	heat flow rate	$\dot{x}$	flow quality	L	liquid
T	temperature	γ	void fraction	b	bulk
U	internal energy	ζ	friction factor	$corr$	correction
V	volume	η	efficiency	a	air
c	specific heat capacity	ρ	density	w	wall
$\underline{h}$	*in situ* specific enthalpy	Ψ	extensive property	f	friction factor
$\bar{h}$	“mixed-cup” specific enthalpy	ψ	intensive property		

REFERENCES

Air Conditioning Library User Guide. Modelon (2014). v1.8.4.

Bauer, O. *Modeling of Two-Phase Flows in Modelica*. Master’s thesis, Lund Institute of Technology (1999).

Bonilla, J., Yebra, L., and Dormido, S. Chattering in dynamic mathematical two-phase flow models. *Applied Mathematical Modeling*, 36:2067–2081 (2012).

Casella, F. Object-oriented modeling of two-phase fluid flows by the finite volume method. In *Proceedings of the 5th MATHMOD Conference* (2006).

Cellier, F. and Kofman, E. *Continuous System Simulation*. Springer (2006).

Elmqvist, H., Tummescheit, H., and Otter, M. Object-oriented modeling of thermo-fluid systems. In *Proceedings of the 3rd Modelica Conference* (2003).

Franke, R., Casella, F., Otter, M., Sielemann, M., Elmqvist, H., Mattson, S.E., and Olsson, H. Stream connectors: An extension of Modelica for device-oriented modeling of convective transport phenomena. In *Proceedings of the 7th Modelica Conference* (2009a).

Franke, R., Casella, F., Sielemann, M., Proelss, K., Otter, M., and Wetter, M. Standardization of thermo-fluid modeling in Modelica.Fluid. In *Proceedings of the 7th Modelica Conference* (2009b).

Ghiaasiaan, S. *Two-Phase Flow, Boiling, and Condensation in Conventional and Miniature Systems*. Cambridge University Press (2007).

Ishii, M. and Hibiki, T. *Thermo-Fluid Dynamics of Two-Phase Flow*. Springer, 2 edition (2011).

Kærn, M. *Analysis of flow maldistribution in fin-and-tube evaporators for residential air-conditioning systems*. Ph.D. thesis, Technical University of Denmark (2011).

Kolev, N. *Multiphase Flow Dynamics 2*. Springer (2005).

Li, P., Li, Y., Seem, J., Qiao, H., Li, X., and Winkler, J. Recent advances in dynamic modeling of HVAC equipment. Part 2: Modelica-based modeling. *HVAC&R Research*, 20(1):150–161 (2014a).

Li, P., Qiao, H., Li, Y., Seem, J., Winkler, J., and Li, X. Recent advances in dynamic modeling of HVAC equipment. Part 1: Equipment modeling. *HVAC&R Research*, 20(1):136–149 (2014b).

Modelica Association. Modelica specification, version 3.3 (2014).

Mortada, S., Zoughaib, A., Clodic, D., and Arzano-Daurelle, C. Dynamic modeling of an integrated air-to-air heat pump using Modelica. *International Journal of Refrigeration*, 35(5):1335–1348 (2012).

Patankar, S. *Numerical Heat Transfer and Fluid Flow*. Hemisphere Publishing Co. (1980).

Rasmussen, B. Dynamic modeling for vapor compression systems. Part 1: Literature review. *HVAC&R Research*, 18(5):934–955 (2012).

Stephan, P., editor. *VDI Heat Atlas*. Springer-Verlag (2010).

White, F. *Fluid Mechanics*. McGraw-Hill, 6 edition (2008).

Willems, J. The behavioral approach to open and interconnected systems. *IEEE Control Systems Magazine*, 27:46–99 (2007).